Characterizing the pathogenic, genomic, and chemical traits of *Aspergillus fischeri*, the closest sequenced relative of the major human fungal pathogen *Aspergillus fumigatus*

Matthew E. Mead[a], Sonja L. Knowles[b], Huzefa A. Raja[b], Sarah R. Beattie[c#], Caitlin H. Kowalski[c], Jacob L. Steenwyk[a], Lilian P. Silva[d], Jessica Chiaratto[d], Laure N.A. Ries[d], Gustavo H. Goldman[d], Robert A. Cramer[c], Nicholas H. Oberlies[b], and Antonis Rokas[a,*]

[a]Department of Biological Sciences, Vanderbilt University, Nashville, Tennessee, USA

[b]Department of Chemistry and Biochemistry, University of North Carolina at Greensboro, Greensboro, North Carolina, USA

[c]Department of Microbiology and Immunology, Geisel School of Medicine at Dartmouth, Hanover, New Hampshire, USA

[d]Faculdade de Ciencias Farmacêuticas de Ribeirão Preto, Universidade de São Paulo, Brazil

Running Title: *Aspergillus fischeri* comparison with *Aspergillus fumigatus*

[*]Address correspondence to Antonis Rokas, Antonis.rokas@vanderbilt.edu

[#] Department of Pediatrics, University of Iowa Carver College of Medicine, Iowa City, Iowa, USA

Keywords: fungal pathogenesis, comparative genomics, and secondary metabolism

Abstract

Aspergillus fischeri is a very close evolutionary relative of the major cause of invasive mold infections, *Aspergillus fumigatus*. In contrast to *A. fumigatus*, *A. fischeri* rarely causes invasive disease, but why such a discrepancy between the species exists is unknown. To begin to address this question, we characterized the pathogenic, genomic, and secondary metabolic similarities and differences between *A. fischeri* and *A. fumigatus*. We observed multiple differences between the two species for phenotypes related to pathogenesis, including that *A. fischeri* is less virulent than *A. fumigatus* in multiple murine models of invasive disease. In contrast, ~90% of the *A. fumigatus* proteome is conserved in *A. fischeri*, including all but one of the previously known *A. fumigatus* genetic determinants important for virulence. However, the two species differed substantially in their biosynthetic gene clusters (BGCs) that are likely involved in the production of secondary metabolites, with only 10 / 33 *A. fumigatus* BGCs also conserved in *A. fischeri*. Detailed chemical characterization of *A. fischeri* cultures grown on multiple substrates identified multiple secondary metabolites, including two new compounds and one never before isolated as a natural product. Interestingly, a deletion mutant in *A. fischeri* of the ortholog of a master regulator of secondary metabolism, *laeA*, produced fewer secondary metabolites and in lower quantities, suggesting that regulation of secondary metabolism is at least partially conserved between the two species. These results suggest that the less-pathogenic *A. fischeri* possesses many of the genes important for *A. fumigatus* pathogenicity but is divergent with respect to its secondary metabolism and its ability to thrive under infection-relevant conditions.

Importance

Aspergillus fumigatus is the primary cause of aspergillosis, a multi-faceted and devastating disease associated with severe morbidity and mortality worldwide. *A. fischeri* is a very close relative of *A. fumigatus*, but it is rarely associated with human disease. To gain insights into the underlying causes of this remarkable difference in pathogenicity, we compared the two organisms for a range of infection-relevant biological and chemical characteristics. We found that disease progression in multiple *A. fischeri* mouse models was much slower and caused less mortality than *A. fumigatus*. The two species also exhibited different growth profiles when placed in a range of infection-relevant conditions, such as low oxygen. Interestingly, we also found that *A. fischeri* contains all but one of the genes previously identified as essential for *A. fumigatus* virulence. However, the two species differ significantly in their secondary metabolic pathways and profiles. The similarities and differences that we identified shed light into the evolutionary origin of a major fungal pathogen.

Introduction

Aspergillosis is a major cause of human morbidity and mortality, resulting in over 200,000 life-threatening infections each year worldwide (1). Aspergillosis is primarily caused by the fungal pathogen *Aspergillus fumigatus* and most commonly affects immunocompromised patients (1). Multiple virulence traits are known for *A. fumigatus*, including thermotolerance, the ability to grow under low oxygen conditions, the ability to acquire micronutrients such as iron and zinc in limiting environments, and the ability to produce a diverse set of secondary metabolites (1, 2).

Thermotolerance is a key trait for survival in a mammalian host and may have arisen from the need of *A. fumigatus* to survive in the warm temperatures present in one of its ecological niches, decaying compost piles (2-4). The primary route of *A. fumigatus* infection is through the lung, where oxygen levels have been observed to be as low as 2/3 of atmospheric pressure, and a successful response to this hypoxic environment is required for pathogenesis (5, 6). *A. fumigatus* produces a diverse set of small molecules, termed secondary metabolites, which are biosynthesized in pathways that exist outside of primary metabolism. Some of these secondary metabolites and their regulators have been shown to be required for disease in mouse models (7-9). For example, when the nonribosomal peptide synthase (*gliP*) required for the production of the secondary metabolite gliotoxin was deleted from *A. fumigatus*, the resulting mutant strain exhibited attenuated virulence in a steroid immune suppression mouse model of aspergillosis but not in leukopenic models (10-13). Furthermore, a master regulator of secondary metabolism, *laeA*, is also required for full virulence in mouse infection studies (14, 15).

Other species closely related to *A. fumigatus* are also capable of causing disease, but they are rarely seen in the clinic (16-19). For example, *A. fischeri* is the closest evolutionary relative to *A. fumigatus* for which a genome has been sequenced 1, but it has only rarely been reported to cause disease (16). *A. fumigatus* is a member of the subgenus *Fumigati*, and while other species in this clade are rarely pathogenic, many of them have been reported to be highly resistant to antifungal drugs (20). Why these closely related species (in the case of *A. fischeri*, it is approximately 93% similar at the protein sequence level to *A. fumigatus* (21)) are unable to cause severe disease in as high of numbers as *A. fumigatus* is an open question. Non-mutually exclusive possibilities include differences in ecological abundance, lack of species level diagnosis in the clinic of disease-causing strains, and innate differences in pathogenicity between section *Fumigati* species and strains.

However, previous studies have suggested that the differences seen in the clinic between species in the subgenus *Fumigati* are unlikely to be due to ecological factors, as several different species in the subgenus are frequently isolated from a variety of locales, including soils, fruits, and hospitals (22-24). For example, approximately 2% of the fungi isolated from the respiratory intensive care unit at Beijing Hospital were *A. fischeri* (compared to approximately 23% of fungal species identified as *A. fumigatus*) (24). Fedorova and collaborators found that when comparing the genomes of *A. fischeri*, *A. fumigatus*, and a more distantly related species (*A. clavatus*), 818 genes were *A. fumigatus*-specific (25). They also reported that the set of *A. fumigatus*-specific genes was enriched for genes involved in carbohydrate transport and catabolism, secondary metabolite biosynthesis, and detoxification relative to the genome as a

whole, suggesting a possible genic source for the pathogenic differences between *A. fumigatus* and *A. fischeri*.

To gain further insight into the differences between the largely non-pathogenic *A. fischeri* and the pathogenic *A. fumigatus*, we took a multi-pronged approach to investigate phenotypic, genomic, and chemical differences between two respective strains of the two species (*A. fischeri* NRRL 181 and *A. fumigatus* CEA10). Our studies revealed that while *A. fischeri* is able to cause fatal disease in multiple mouse models of *Aspergillus* infection, its disease progression and response to multiple disease-relevant stresses is markedly different than that of the *A. fumigatus* strain examined. We also found that *A. fischeri* substantially differed from *A. fumigatus* in its secondary metabolite profile and secondary metabolite gene clusters, even though the regulation of secondary metabolism by *laeA* in *A. fischeri* closely resembled what has been observed in *A. fumigatus*.

Results

A. fischeri is significantly less virulent than *A. fumigatus* in multiple animal models of Invasive Pulmonary Aspergillosis (IPA).

Only a handful of cases of invasive fungal infections caused by *A. fischeri* have been reported in the literature (26-29). Given the scarcity of these infections as compared to *A. fumigatus*, we utilized two immunologically distinct murine IPA models to assess differences in virulence between the two species. In a leukopenic model, *A. fischeri* NRRL181 is significantly less virulent than *A. fumigatus* CEA10, in a dose dependent manner (Fig. 1). Using an inoculum of $1x10^5$ conidia, *A. fischeri* is completely attenuated in virulence, with 100% murine survival by

day 15 post-fungal challenge. In contrast, inoculation with *A. fumigatus* results in 100% murine mortality by day 15 (Fig. 1A). Using a higher dose ($2x10^6$) of conidia, both strains cause 90% mortality by day 14, however, the disease progression is markedly different. 80% of mice inoculated with *A. fumigatus* succumb to infection by day 4, whereas for mice inoculated with *A. fischeri*, the first mortality event occurs on day 5, and then one or two mice succumb each day until day 14 (Fig. 1B). Thus, despite the similar overall mortality at higher fungal challenge doses, *A. fischeri* is significantly less virulent in this model. As the patient population at risk for invasive aspergillosis continues to change (30), we also tested a non-neutropenic triamcinolone (steroid)-induced immune suppression model and observed a significant reduction in virulence of *A. fischeri* compared to *A. fumigatus* ($p<0.0001$ by Log-Rank and Gehan-Breslow-Wilcoxon tests). Mice inoculated with *A. fumigatus* all succumbed to infection by day 3; however, similar to the neutropenic model, animals inoculated with *A. fischeri* had a slower disease progression (Fig. 1C). We observed similar results when using the *Galleria mellonella* insect larvae model of aspergillosis infection (Fig. 1EF). Both low ($1x10^6$ conidia) and high ($1x10^9$ conidia) inoculum experiments showed significant differences between the disease progression of *A. fischeri* and *A. fumigatus*.

To better understand what is happening *in vivo* during infection with *A. fischeri* and *A. fumigatus*, we performed histological analysis on lungs from the triamcinolone model 3 days post inoculation. Histological sections were stained with Gomori methenamine silver (GMS) to visualize fungal growth and hematoxylin and eosin (H&E) stain to visualize host cell infiltration (Fig. 1D). Overall, mice inoculated with *A. fischeri* had similar numbers of fungal lesions to those inoculated with *A. fumigatus* but the lesions caused by the two species were phenotypically

147 distinct. In large airways infected with *A. fumigatus*, there was greater fungal growth per lesion,
148 and the growth was observed throughout the major airway itself. These lesions are accompanied
149 by inflammation, which appears largely neutrophilic and obstructs the airways surrounding the
150 hyphae. In the lesions containing *A. fischeri*, the fungal growth is contained to the epithelial
151 lining of the airways. This pattern of growth is accompanied by inflammation at the airway
152 epithelia, leaving the large airways largely unobstructed. The lack of airway obstruction during
153 *A. fischeri* infection may contribute to the reduced virulence compared to *A. fumigatus*.
154
155 Although the distribution of the fungal lesions varies, there is still significant fungal
156 growth in these animals, suggesting that *A. fischeri* is capable of growing within the host. Indeed,
157 we tested the growth rate of *A. fischeri* and *A. fumigatus* in lung homogenate as a proxy for
158 growth capability within the nutrient environment of the host and observed no difference
159 between the two strains (Fig. S1). These experiments show that in two murine models of IPA, *A.*
160 *fischeri* is less virulent than *A. fumigatus*, although *A. fischeri* is still capable of causing disease
161 using a higher dose and importantly, is able to grow within the murine host.
162
163 <u>*A. fischeri* is more susceptible to several infection-relevant stresses than *A. fumigatus*</u>
164 Our *in vivo* experiments suggested that the attenuation of virulence is not solely a result
165 of the inability of *A. fischeri* to grow within the host, therefore we hypothesized that the inability
166 to mitigate host stress is a contributing factor to the virulence defects. Nutrient fluctuation is a
167 stress encountered *in vivo* during *A. fumigatus* infection (31). To assess differences in metabolic
168 plasticity between the two strains, growth was measured on media supplemented with glucose,
169 fatty acids (Tween-80), or casamino acids. Because low oxygen tension is a significant stress

encountered during infection (5), and recently, fitness in low oxygen has been correlated to virulence of *A. fumigatus* (32), we measured growth of both strains at 37°C in both normoxic (ambient air) and hypoxia-inducing (0.2% O_2, 5% CO_2) conditions. In normoxia with glucose, fatty acids (Tween-80), or casamino acids supplied as the carbon source, radial growth of *A. fischeri* was lower than that of *A. fumigatus*. However, on rich media both strains grew equally well (Fig. 2). We also observed a slower growth rate of *A. fischeri* compared to *A. fumigatus* in the first 16 hours of culture in liquid media supplied with glucose at 37°C. At 30°C *A. fischeri* grew the same as, or better than, *A. fumigatus* except on Tween-80 where *A. fumigatus* has a slight advantage (Fig. S2). Also, *A. fischeri* grew substantially worse than *A. fumigatus* when grown at 44°C (Fig. S3). To determine relative fitness in hypoxic liquid environments, we measured the ratio of biomass in liquid culture in ambient air (normoxia) versus hypoxic (0.2% O_2, 5%CO_2) conditions. *A. fischeri* showed significantly lower fitness in hypoxia, with about an 8.5-fold lower biomass than *A. fumigatus* (Fig. 3A). These data suggest that *A. fischeri* is less fit than *A. fumigatus* at 37°C and in low oxygen conditions, both of which have been shown to impact fungal virulence.

Metabolic flexibility, or the ability for an organism to utilize multiple carbon sources simultaneously, has been suggested to provide a fitness advantage to *Candida albicans* during *in vivo* growth (33). Metabolic flexibility can be characterized using the glucose analog, 2-deoxyglucose (2-DG), in combination with an alternative carbon source available *in vivo* such as lactate. 2-DG triggers carbon catabolite repression, which shuts down alternative carbon utilization pathways. However, in *C. albicans* this shut down is delayed and growth occurs on lactate with 2-DG (33, 34). We tested this phenomenon in both *A. fumigatus* and *A. fischeri* and

193 observed that while both strains can grow in the presence of 2-DG on lactate, growth of *A.*
194 *fischeri* is more inhibited under these conditions (~60%) compared to *A. fumigatus* (~35%; Fig.
195 3B). Even under low oxygen conditions (5% and 2%), *A. fumigatus* maintains this metabolic
196 flexibility except under extremely low oxygen conditions (0.2%), whereas *A. fischeri* is even
197 more inhibited at all oxygen tensions of 5% or below. Thus, these data suggest that while both
198 species exhibit some level of metabolic flexibility, *A. fumigatus* appears more metabolically
199 flexible under a wider range of conditions than *A. fischeri*.
200
201 Next, we measured the susceptibility of *A. fischeri* to oxidative stress, cell wall stress, and
202 antifungal drugs. Interestingly, we observed that *A. fischeri* is more resistant to the intracellular
203 generating oxidative stress agent menadione than *A. fumigatus* and is more susceptible to
204 external oxidative stress agent H_2O_2 than *A. fumigatus* (Fig. 3CD). As levels of inflammation
205 appeared different between the species *in vivo*, we indirectly tested for differences in cell wall
206 pathogen associated molecular patterns using cell wall perturbing agents Congo Red and
207 Calcofluor White. For both of these agents, *A. fumigatus* was significantly more resistant than *A.*
208 *fischeri* suggesting differences in the response to cell wall stress or in the composition and
209 organization of the cell wall (Fig. 3C). This is especially important for host immune cell
210 recognition and interaction and will influence pathology and disease outcome. Lastly, *A. fischeri*
211 showed enhanced resistance relative to *A. fumigatus* for three of the four antifungal drugs tested
212 (Table 1), similar to what has been shown in the past (35). Overall, our phenotypic data show
213 variability in the response of *A. fischeri* to host-related stresses and antifungals. Increased growth
214 capability in low oxygen and thermotolerance are two important attributes that likely contribute
215 to the success of *A. fumigatus* as a pathogen compared to *A. fischeri*.

The genomes of *A. fumigatus* and *A. fischeri* are highly similar, but their secondary metabolite cluster genes are divergent

The large differences in virulence and virulence-related traits we observed between *A. fumigatus* and *A. fischeri* led us to investigate the genotypic differences that could be responsible. To describe the genomic similarities and differences between *A. fumigatus* and *A. fischeri*, we determined how many orthologous proteins and how many species-specific proteins were present in each genome using a Reciprocal Best BLAST Hit approach (36). We identified 8,737 proteins as being shared between the two species (Fig. S4), representing 88% and 84% of the *A. fumigatus* and *A. fischeri* genomes, respectively. To narrow our search for genes that are absent in *A. fischeri* but are important for *A. fumigatus* disease, we classified 49 *A. fumigatus* genes as being genetic determinants important for virulence (Table S1) based on two previously published articles (37, 38) and extensive literature searches of our own. We observed that all but one of these pathogenicity- and virulence-associated genes were also present in *A. fischeri*, a surprising finding considering the substantial differences observed between the two species in our mouse models of infection. The virulence-associated gene not present in *A. fischeri* is *pesL* (Afu6g12050), a non-ribosomal peptide synthase that is essential for the synthesis of the secondary metabolite fumigaclavine C and required for virulence in the *G. mellonella* model of *A. fumigatus* infection (22, 23).

Since the only previously described *A. fumigatus* virulence associated gene not present in the *A. fischeri* genome (i.e. *pesL*) is also involved in biosynthesizing the ergot alkaloid fumigaclavine C, we investigated the differences between the repertoire of secondary metabolite

cluster genes present in *A. fumigatus* and *A. fischeri*. Using the program antiSMASH (39) we identified 598 secondary metabolic cluster genes distributed amongst 33 clusters in *A. fumigatus* strain CEA10 (Table S2) and 786 secondary metabolite cluster genes spread out over 48 clusters in *A. fischeri* strain NRRL 181 (Table S3). Of the 598 secondary metabolic cluster genes we identified in *A. fumigatus*, 407 of them had an ortholog that was also in an *A. fischeri* secondary metabolic gene cluster. This level of conservation between secondary metabolic cluster genes (68%) is much lower than the amount of conservation seen when considering proteins from the entire genome (88%), illustrating the rapid rate at which these metabolic pathways and genomic architectures can change and evolve.

We next sought to directly compare the list of *A. fischeri* secondary metabolic gene clusters to the list of secondary metabolic gene clusters from *A. fumigatus*. An *A. fumigatus* gene cluster was considered conserved in *A. fischeri* if 90% or more of its genes were also in an *A. fischeri* gene cluster. Only 10 out of the 33 *A. fumigatus* gene clusters are conserved in *A. fischeri* (Fig. 4), confirming our individual gene-based findings that secondary metabolism in *A. fumigatus* and *A. fischeri* is quite different.

While only 10 *A. fumigatus* gene clusters were conserved in *A. fischeri*, many others possessed at least one ortholog that could be found in an *A. fischeri* secondary metabolic gene cluster. However, one gene cluster (Cluster 18) was completely *A. fumigatus*-specific (i.e. it did not have any orthologs in the *A. fischeri* secondary metabolic gene clusters or in the rest of the *A. fischeri* genome), and antiSMASH predicted this gene cluster to produce a terpene-based metabolite. Our search for *A. fumigatus* virulence factors in *A. fischeri* revealed that *pesL*, the

NRPS from the fumigaclavine biosynthetic pathway, was not present in *A. fischeri*, and our expanded gene cluster search showed that only one gene from the entire fumigaclavine gene cluster is present in *A. fischeri,* again suggesting that fumigaclavine production is likely not present in *A. fischeri*. In addition, there are 10 *A. fischeri* gene clusters that do not have any orthologs in secondary metabolic gene clusters in *A. fumigatus*. One of these *A. fischeri*-specific gene clusters is responsible for making helvolic acid (a gene cluster known to be absent from the *A. fumigatus* strain CEA10 but present in strain Af293 (40)), while the other 9 have not been biochemically connected to any metabolite.

Our analyses also showed that all the genes required for the production of the mycotoxin gliotoxin (a mycotoxin) are located in a gene cluster in *A. fischeri* (Fig. S5), and are in fact very similar to their *A. fumigatus* orthologs (41). *A. fumigatus* and *A. fischeri* gliotoxin cluster gene orthologs share on average approximately 94% of their protein sequences, a level of similarity comparable to that exhibited between all reciprocal best blast hit pairs in *A. fumigatus* and *A. fischeri* (93%). However, the *A. fischeri* copy of GliZ (Afu6g09630), the cluster-specific regulator of gliotoxin production in *A. fumigatus*, only shared 78% of its protein sequence with its *A. fischeri* counterpart. It is thus possible that differences in how gliotoxin cluster genes are regulated in the two species could be responsible for why *A. fischeri* is not known to produce this mycotoxin (42).

Both the gliotoxin and acetylaszonalenin gene clusters are located immediately next to one another (Fig. S5) in *A. fischeri*. In *A. fumigatus*, the gliotoxin gene cluster is immediately next to what appears to be a version of the acetylaszonalenin cluster that is lacking portions of the

nonribosomal peptide synthase and acetyltransferase and the entire indole prenyltransferase required for acetylaszonalenin production. The close proximity of these two gene clusters is noteworthy, as it is another example of a rapidly evolving "super cluster" in *A. fumigatus* and *A. fumigatus*-related strains (43). These super clusters have been hypothesized to be "evolutionary laboratories" that may give rise to new compounds and pathways (40).

Isolation and characterization of three new compounds from *A. fischeri*

The relatively low level of conservation we observed at the genomic loci likely responsible for secondary metabolism in *A. fumigatus* and *A. fischeri* led us to characterize the secondary metabolites *A. fischeri* produced using solid state fermentation with commercially available rice, followed by extraction and purification via HPLC (Fig. S6) (44-48). The fractions from the solid-state culture yielded three known compounds, sartorypyrone A (**1**), aszonalenin (**4**), and acetylaszonalenin (**5**) (Fig. 5A). To better explore the chemical diversity of *A. fischeri*, the one strain-many compounds (OSMAC) approach was used to alter the secondary metabolites being biosynthesized (49-52). *A. fischeri* was subsequently grown on multigrain cheerios and yielded the three secondary metabolites from rice (**1**, **4**, and **5**), and four additional secondary metabolites fumitremorgin A (**6**), fumitremorgin B (**7**), verruculogen (**8**), and the C-11 epimer of verruculogen TR2 (**9**). These results suggest that culture media influences the biosynthesis of secondary metabolites in *A. fischeri* as observed in many other fungi (50, 53).

To further explore the effect of culture conditions on secondary metabolism in *A. fischeri*, secondary metabolite production was evaluated in a suite of growth conditions, including both synthetic and rich media (Figs. 5B and S7 and Table S4) and the chemical profile was assessed

by Liquid Chromatography-Mass Spectrometry (LC-MS). The analysis showed that oatmeal agar (OMA) produced chromatographic peaks that were not seen in any other growth media. This finding prompted a scale-up to characterize the peaks of interest. This process yielded the seven previously isolated compounds (**1** and **4**-**9**) and three newly biosynthesized secondary metabolites (**2**, **3**, and **10**). Two of the secondary metabolites were new compounds (sartorypyrone E (**2**) and 14-epi-aszonapyrone A (**3**)) and one was a new natural product (13-*O*-prenyl-fumitremorgin B (**10**)) (Fig. 5B). The structures were determined using a set of spectroscopic (1 and 2D NMR) and spectrometric techniques (HRMS). Our data for sartorypyrone A (**1**) (54), aszonalenin (**4**) (55, 56), acetylaszonalenin (**5**) (54, 57), fumitremorgin A (**6**) (58, 59), fumitremorgin B (**7**) (60-62), verruculogen (**8**) (63, 64), and the C-11 epimer of verruculogen TR2 (**9**) (64) correlated well with literature values. The structures of 14-epi-aszonapyrone A (**3**), and 13-*O*-prenyl fumitremorgin B (**10**) were fully characterized in this study (see Figshare document: https://doi.org/10.6084/m9.figshare.7149167.v1); the structure elucidation of sartorypyrone E (**2**) is ongoing and will be reported in detail in a forth coming manuscript in the organic chemistry literature.

Since four secondary metabolites (**5**-**8**) from *A. fischeri* had also been reported from *A. fumigatus*, we hypothesized that the mechanisms *A. fischeri* employs to regulate its secondary metabolism would also be similar to those used by *A. fumigatus*. To test this hypothesis, we constructed deletion mutants of *laeA* in *A. fischeri* (Fig. S8). LaeA is a master regulator of secondary metabolism in *A. fumigatus* and a variety of other fungi (65-67). Both the wild type and Δ*laeA* strains were subjected to LC-MS analysis at a concentration of 2.0 mg/mL, and with a gradient starting at 15% CH_3CN and linearly increasing to 100% CH_3CN over 8 minutes. The

chromatographic profile of Δ*laeA* showed mass data that corresponded to sartorypyrone A (**1**), sartorypyrone E (**2**), 14-epi-aszonapyrone A (**3**), aszonalenin (**4**), acetylaszonalenin (**5**), fumitremorgin A (**6**), verruculogen (**8**), and the C-11 epimer of verruculogen TR2 (**9**). However, the relative abundance of compounds present was very low compared to the wild type (Fig. 5C). Fumitremorgin B (**7**) and 13-*O*-prenyl-fumitremorgin B (**10**) were not produced by the Δ*laeA* mutant at all.

Discussion

A. fumigatus is an important human fungal pathogen, yet other closely related species in the subgenus *Fumigati* are either unable to cause disease or do so in very low frequencies. A number of traits that contribute to the virulence of *A. fumigatus* have been characterized, but their distribution and potential role in affecting the less prevalent diseases caused by other section *Fumigati* species is largely unknown. To begin to study how *A. fumigatus* pathogenicity may be different from the pathogenicities of other section *Fumigati* species, we thoroughly characterized *A. fischeri*, the closest sequenced relative of *A. fumigatus*, for multiple disease-relevant biological and chemical differences.

Our data suggested that *A. fischeri* strain NRRL 181 is able to grow in a mammalian host but is much less fit than *A. fumigatus* strain CEA10. Consequently, phenotypic analyses of a single strain of each species revealed significant differences in their ability to adapt to known pathogenesis-related stress environments including low oxygen, oxidative stress-inducing agents, and cell wall perturbing molecules. Moreover, basic differences in the growth of the two organisms at multiple temperatures and under multiple diverse nutrient conditions revealed

354 fundamental metabolic differences between these two strains and species. These differences in
355 disease-relevant traits led us to look for the genomic attributes that were responsible for them.
356 The only *A. fumigatus* gene required for virulence that was missing from *A. fischeri* was a gene
357 encoding a nonribosomal peptide synthase required for fumigaclavine C biosynthesis (Table S1).
358 Fumigaclavine C biosynthesis is required for *A. fumigatus* pathogenicity (68) and is a potent
359 anti-inflammatory (69). We were surprised to see an anti-inflammatory gene missing in *A.*
360 *fischeri* considering our histology data suggests that *A. fumigatus* recruits more inflammatory
361 cells to sites of fungal lesions. However, additional quantitative analyses of the host immune
362 response to these species is needed, and multiple factors contribute to the development of
363 inflammation and host damage during infection including, but not limited to, fungal secondary
364 metabolites. In addition, O'Hanlon et al. reported that the loss of *pesL* in *A. fumigatus* resulted in
365 increased production of fumitremorgins; compounds similar or identical to those were isolated
366 during our chemical study (Fig 5AB).
367
368 Further investigations into the conservation and divergence of secondary metabolic gene
369 clusters in *A. fischeri* and *A. fumigatus* revealed that secondary metabolic genes are much less
370 conserved than genes in the rest of the genome. This finding is consistent with our previous
371 results showing that secondary metabolism is a dynamic process that evolves quickly between
372 closely related species or even between strains of the same species (40, 70). Ten gene clusters
373 were *A. fischeri*-specific (i.e. they did not possess orthologs in the list of secondary metabolic
374 cluster genes present in *A. fumigatus*) (Fig 3.), implying that they were either gained by *A.*
375 *fischeri* or lost by *A. fumigatus*. A further examination of the secondary metabolic cluster gene

repertoire in other section *Fumigati* species is needed to discern the evolutionary pattern of these "*A. fischeri*-specific" gene clusters.

Cluster 18 was the only gene cluster found to be *A. fumigatus*-specific and contains an uncharacterized squalene-hopene cyclase, a class of enzymes that contribute to the production of molecules important for membrane fluidity in Bacteria (71). The presence of the small molecule produced by Cluster 18 in the membrane of *A. fumigatus* could contribute to its ability to evade the host immune system and/or be less susceptible to the infection-relevant stresses we tested relative to *A. fischeri*.

We report here for the first time two compounds isolated from *A. fischeri* (sartorypyrone E (**2**) and 14-epi-aszonapyrone (**3**)) in addition to the first natural production of 13-*O*-prenyl-fumitremorgin B (**10**). 13-*O*-prenyl-fumitremorgin B was previously produced *in vitro* using purified fumitremorgin B, dimethylallyl pyrophosphate, and the prenyltransferase FtmPT3 (NFIA_093400) (62), but this is the first report of its natural production and isolation from *A. fischeri*. Interestingly, FtmPT3 is not located in the previously described fumitremorgin cluster (72) but is located relatively near it in another predicted antiSMASH cluster (Cluster 9).

LaeA is a master regulator of secondary metabolism in a diverse set of organisms (65, 67, 73), and we have shown here that it functions similarly in *A. fischeri* (Fig. 5C). Every metabolite we isolated from the wild type strain decreased in abundance in the Δ*laeA* strain, and fumitremorgin B (**7**) and 13-*O*-prenyl-fumitremorgin B (**10**) were not produced by the mutant at all. Our data matches reports of *laeA* regulating fumitremorgin production in *A. fumigatus* (15,

399 74) and suggests at least a partially conserved network of *laeA* regulation in *A. fischeri*.
400 Furthermore, our finding that *laeA* regulates the acetylaszonalenin cluster shows that this
401 important gene controls the production of global secondary metabolism in *A. fischeri* and not
402 only orthologs of the targets of *laeA* from *A. fumigatus*.
403
404 Together, our data suggests that *A. fischeri* is less virulent in murine models of infection
405 than its closest sequenced relative, *A. fumigatus*, despite significant conservation between their
406 genomes. Based on our results, we hypothesize that the decrease in virulence of *A. fischeri*
407 relative to *A. fumigatus* is due at least in part to differences in the ability of the two organisms to
408 respond to pathogenesis-relevant stresses and their different secondary metabolite profiles. The
409 differences in the pathobiology traits between these two species warrant further investigation,
410 especially as the appreciation for the health burden caused by species in the subgenus Fumigati
411 increases. An important future direction is to expand these studies to include larger numbers of
412 strains and species from section Fumigati in order to fully appreciate the biological and genetic
413 diversity in this important subgenus. Leveraging this diversity will allow us to better understand
414 the nature and evolution of human fungal pathogenesis.
415
416 **Materials and Methods**
417 Strains and growth media
418 *A. fischeri* strain NRRL 181 was acquired from the ARS Culture Collection (NRRL). All
419 strains were maintained on glucose minimal media (GMM) from glycerol stocks stored at -80°C.
420 All strains were grown in the presence of white light at 37°C. Conidia were collected in 0.01%
421 Tween-80 and enumerated with a hemocytometer.

422

423 Murine virulence studies

424 For the chemotherapeutic (leukopenic) murine model, outbred CD-1 female mice
425 (Charles River Laboratories, Raleigh, NC, USA), 6-8 weeks old, were immunosuppressed with
426 intraperitoneal (i.p.) injections of 150 mg/kg cyclophosphamide (Baxter Healthcare Corporation,
427 Deerfield, IL, USA) 48 hours before and 72 hours after fungal inoculation, along with
428 subcutaneous (s.c.) injections of 40 mg/kg Kenalog-10 (triamcinolone acetonide, Bristol-Myer
429 Squibb, Princeton, NJ, USA) 24 hours before and 6 days after fungal inoculation. For the murine
430 triamcinolone model outbred CD-1 female mice, 6-8 weeks old, were treated with 40 mg/kg
431 Kenalog-10 by s.c. injection 24 hours prior to fungal inoculation.

432

433 For both models, conidial suspensions of $2x10^6$ conidia were prepared in 40 µL sterile
434 PBS and administered to mice intranasally while under isoflourine anesthesia. Mock mice were
435 given 40 µL PBS. Mice were monitored three times a day for signs of disease for 14 or 18 days
436 post-inoculation. Survival was plotted on Kaplan-Meir curves and statistical significance
437 between curves was determined using Mantel-Cox Log-Rank and Gehan Breslow-Wilcoxon
438 tests. Mice were housed in autoclaved cages at 4 mice per cage with HEPA filtered air and
439 autoclaved food and water available at libitum.

440

441 *G. mellonella* virulence studies

442 *G. mellonella* larvae were obtained by breeding adult moths (Fuchs *et al.*, 2010). *G.*
443 *mellonella* larvae of a similar size were selected (approximately 275–330 mg) and kept without
444 food in glass container (Petri dishes), at 37°C, in darkness for 24 h prior to use. *A. fumigatus and*

445 *A. fischeri* conidia were obtained by growing on YAG media culture for 2 days. The conidia
446 were harvested in PBS and filtered through a Miracloth (Calbiochem). The concentration of
447 conidia was estimated by using hemocytometer, and resuspended at a concentration of 2.0 x 10^8
448 conidia/ml. The viability of the conidia was determined by incubating on YAG media culture, at
449 37°C, 48 hours. Inoculum (5 µl) of conidia from both strains were used to investigate the
450 virulence of *A. fumigatus* and *A. fischeri* against *G. mellonella*. Ten *G. mellonella* in the final
451 (sixth) instar larval stage of development were used per condition in all assays. The control
452 group was the larvae inoculated with 5 µl of PBS to observe the killing due to physical trauma.
453 The inoculum was performed by using Hamilton syringe (7000.5KH) and 5 µl into the haemocel
454 of each larva via the last left proleg. After, the larvae were incubated in glass container (Petri
455 dishes) at 37ºC in the dark. The larval killing was scored daily. Larvae were considered dead by
456 presenting the absence of movement in response to touch.

457

458 Histopathology

459 Outbred CD-1 mice, 6-8 weeks old, were immunosuppressed and intranasally inoculated
460 with 2x10^6 conidia as described above for the chemotherapeutic and corticosteroid murine
461 models. Mice were sacrificed 72 hours post inoculation. Lungs were perfused with 10% buffered
462 formalin phosphate before removal, then stored in 10% buffered formalin phosphate until
463 embedding. Paraffin embedded sections were stained with haematoxylin and eosin (H&E) and
464 Gömöri methenamine silver (GMS). Slides were analyzed microscopically with a Zeiss Axioplan
465 2 imaging microscope (Carl Zeiss Microimaging, Inc. Thornwood, NY, USA) fitted with a
466 Qimiging RETIGA-SRV Fast 1394 RGB camera. Analysis was performed in Phylum Live 4
467 imaging software.

468

469 Ethics Statement

470 We carried out our animal studies in strict accordance with the recommendations in the
471 Guide for the Care and Use of Laboratory Animals of the National Research Council (Council,
472 1996). The animal experimental protocol was approved by the Institutional Animal Care and Use
473 Committee (IACUC) at Dartmouth College (Federal-Wide Assurance Number: A3259-01).

474

475 Growth Assays

476 Radial growth was quantified by point inoculation of $1x10^3$ conidia in 2µL on indicated
477 media; plates were incubated at 37°C in normoxia (~21% O_2, 5% CO_2) or hypoxia (0.2% O_2, 5%
478 CO_2). Colony diameter was measured every 24 hours for 4 days and reported as the average of
479 three biological replicates per strain.

480

481 For 2-DG experiments, $1x10^3$ conidia in 2 uL were spotted on 1% lactate minimal media
482 with or without 0.1% 2-deoxyglucose (2-DG; Sigma, D8375). Plates were incubated for 3 days
483 at 37°C in normoxia or hypoxia with 5% CO_2. Percent inhibition was calculated by dividing
484 radial growth on 2-DG plates by the average radial growth of biological triplicates on plates
485 without 2-DG.

486

487 Fungal biomass was quantified by measuring the dry weight of fungal tissue from $5x10^7$
488 conidia grown in 100 mL liquid GMM shaking at 200 rpm for 48 hours in normoxia (~21% O_2)
489 and hypoxia (0.2% O_2, 5% CO_2). Liquid biomass is reported as the average of three biological

490 replicates per strain. Hypoxic conditions were maintained using an INVIVO$_2$ 400 Hypoxia
491 Workstation (Ruskinn Technology Limited, Bridgend, UK) with a gas regulator and 94.8% N_2.
492
493 Liquid growth curves were performed with conidia adjusted to $2x10^4$ conidia in 20 µL
494 0.01% Tween-80 in 96-well dishes, then 180 µL of media (GMM or lung homogenate) was
495 added to each well. Plates were incubated at 37°C for 7 hours, then Abs_{405} measurements were
496 taken every 10 minutes for the first 16 hours of growth with continued incubation at 37°C. Lung
497 homogenate media was prepared as follows: lungs were harvested from healthy CD-1 female
498 mice (20-24 g) and homogenized through a 100 µM cell strainer in 2 mL PBS/lung. Homogenate
499 was diluted 1:4 in sterile PBS, spun down to remove cells, then filter sterilized through 22 µM
500 PVDF filters.
501
502 Cell wall and oxidative stresses
503 Congo Red (0.5 mg/mL), Menadione (20 µM), or calcofluor white (CFW, 25 µg/mL)
504 were added to GMM plates. $1x10^3$ conidia (Calcofluor white and Menadione) or $1x10^5$ conidia
505 (Congo Red) were point inoculated and plates were incubated for 96 hours at 37°C with 5% CO_2.
506
507 Orthology Determination and Analyses
508 To identify putative orthologous genes (hence forth referred to as orthologs) between *A.*
509 *fischeri* and *A. fumigatus*, a reciprocal best BLAST hit (RBBH) approach was used. We blasted
510 the proteome of *A. fischeri* to *A. fumigatus* and vice versa using an e-value cutoff of 10^{-3} and then
511 filtered for RBBHs according to bitscore (75). A pair of genes from each species was considered

512 orthologous if their best blast hit was to each other. Species-specific and orthologous protein sets
513 were visualized using version 3.0.0 of eulerAPE (76).
514
515 Enriched Gene Ontology annotations were identified in gene lists using the tools
516 available at FungiDB (77) (accessed on July 25, 2018), and lists were collapsed using the
517 "Small" setting in REVIGO (78).
518
519 Secondary Metabolism Cluster Prediction and Analyses
520 Version 4.2.0 of antiSMASH (39) was used with its default settings to identify secondary
521 metabolite clusters. Orthologous cluster genes were identified using our RBBH results and
522 visualized using version 0.69 of Circos (79). Syntenic clusters were visualized using easyfig
523 version 2.2.2 (80).
524
525 Secondary Metabolite Extraction and Identification
526 Secondary metabolites were extracted from *A. fischeri* using techniques well established
527 in Natural Product literature (81, 82). This was done by adding a 1:1 mixture of $CHCl_3$:CH_3OH
528 and left to shake overnight. The resulting slurry was partitioned twice, first with a 4:1:5
529 $CHCl_3$:CH_3OH:H_2O solution, with the organic layer drawn off and evaporated to dryness *in*
530 *vaccuo,* and secondly reconstituting 1:1:2 CH_3CN:CH_3OH:hexanes, where the organic layer was
531 drawn off and evaporated to dryness. The extract then underwent chromatographic separation
532 (flash chromatography and HPLC) using varied gradient systems. The full structural
533 characterization of the new secondary metabolites is provided in the Figshare document
534 (https://doi.org/10.6084/m9.figshare.7149167.v1).

535

536 Construction of the *A. fischeri* Δ*laeA* mutant

537 The gene replacement cassettes were constructed by ‘‘*in vivo*’’ recombination in *S.*
538 *cerevisiae* as previously described by (83, 84). Approximately 2.0 kb from the 5’-UTR and 3’-
539 UTR flanking regions of the targeted ORF regions were selected for primer design. The primers
540 pRS NF010750 5´fw (5´-
541 GTAACGCCAGGGTTTTCCCAGTCACGACGCAGTCTAACGCTGGGCCCTTCC-3´) and
542 pRS NF010750 3´rv (5´-
543 GCGGTTAACAATTTCTCTCTGGAAACAGCTACGGCGTTTGACGGCACAC-3´) contained
544 a short homologous sequence to the Multicloning site (MCS) of the plasmid pRS426. Both the
545 5’- and 3’-UTR fragments were PCR-amplified from *A. fischeri* genomic DNA (gDNA). The
546 *prtA* gene, conferring resistance to pyrithiamine, which was placed within the cassette as a
547 dominant marker, was amplified from the pPRT1 plasmid by using the primers prtA NF010750
548 5´rv (5´-GTAATCAATTGCCCGTCTGTCAGATCCAGGTCGAGGAGGTCCAATCGG-3´)
549 and prtA NF010750 3´fw (5´-
550 CGGCTCATCGTCACCCCATGATAGCCGAGATCAATCTTGCATCC-3´). The deletion
551 cassette was generated by transforming each fragment along with the plasmid pRS426 cut with
552 *Bam*HI/*Eco*RI into the *S. cerevisiae* strain SC94721, using the lithium acetate method (85). The
553 DNA from the transformants was extracted by the method described by Goldman et al. (86). The
554 cassette was PCR-amplified from these plasmids utilizing TaKaRa Ex Taq™ DNA Polymerase
555 (Clontech Takara Bio) and used for *A. fisheri* transformation according to the protocol described
556 by Malavazi and Goldman (84). Southern blot and PCR analyses were used to demonstrate that
557 the cassette had integrated homologously at the targeted *A. fischeri* locus. Genomic DNA from

A. fischeri was extracted by grinding frozen mycelia in liquid nitrogen and then gDNA was extracted as previously described (84). Standard techniques for manipulation of DNA were carried out as described (87). For Southern blot analysis, restricted chromosomal DNA fragments were separated on 1% agarose gel and blotted onto Hybond N^+ nylon membranes (GE Healthcare). Probes were labeled using [α-^{32}P]dCTP using the Random Primers DNA Labeling System (Life Technologies). Labeled membranes were exposed to X-ray films, which were scanned for image processing. Southern blot and PCR schemes are shown in Fig. S8.

Acknowledgements

Computational infrastructure was provided by The Advanced Computing Center for Research and Education (ACCRE) at Vanderbilt University. MEM, JS, and AR were supported by a Vanderbilt University Discovery Grant. RAC holds an Investigator in the Pathogenesis of Infectious Diseases Award supported by the Burroughs Wellcome Fund (BWF) and is also supported by a National Institute of Allergy and Infectious Diseases (NIAID) award 1R01AI130128. SRB was supported, in part, by the National Institute of General Medical Sciences of the National Institutes of Health under Award Number T32GM008704. SLK was supported by the National Center for Complementary and Integrative Health, a component of the National Institutes of Health, under award number T32 AT008938.

References

1. **Latgé JP**. 1999. Aspergillus fumigatus and aspergillosis. Clin Microbiol Rev **12**:310–350.

2. **Tekaia F**, **Latgé J-P**. 2005. Aspergillus fumigatus: saprophyte or pathogen? Current Opinion in Microbiology **8**:385–392.

3. **Bhabhra R**, **Miley MD**, **Mylonakis E**, **Boettner D**, **Fortwendel J**, **Panepinto JC**, **Postow M**, **Rhodes JC**, **Askew DS**. 2004. Disruption of the Aspergillus fumigatus gene encoding nucleolar protein CgrA impairs thermotolerant growth and reduces virulence. Infect Immun **72**:4731–4740.

4. **Wagener J**, **Echtenacher B**, **Rohde M**, **Kotz A**, **Krappmann S**, **Heesemann J**, **Ebel F**. 2008. The Putative α-1,2-Mannosyltransferase AfMnt1 of the Opportunistic Fungal Pathogen Aspergillus fumigatusIs Required for Cell Wall Stability and Full Virulence. Eukaryotic Cell **7**:1661–1673.

5. **Grahl N**, **Puttikamonkul S**, **Macdonald JM**, **Gamcsik MP**, **Ngo LY**, **Hohl TM**, **Cramer RA**. 2011. In vivo hypoxia and a fungal alcohol dehydrogenase influence the pathogenesis of invasive pulmonary aspergillosis. PLoS Pathog **7**:e1002145.

6. **Willger SD**, **Puttikamonkul S**, **Kim K-H**, **Burritt JB**, **Grahl N**, **Metzler LJ**, **Barbuch R**, **Bard M**, **Lawrence CB**, **Cramer RA**. 2008. A sterol-regulatory element binding protein is required for cell polarity, hypoxia adaptation, azole drug resistance, and virulence in Aspergillus fumigatus. PLoS Pathog **4**:e1000200.

7. **Rokas A**, **Wisecaver JH**, **Lind AL**. 2018. The birth, evolution and death of metabolic gene clusters in fungi. Nature Reviews Microbiology **163**:150.

8. **Keller NP**, **Turner G**, **Bennett JW**. 2005. Fungal secondary metabolism — from biochemistry to genomics. Nature Reviews Microbiology **3**:937–947.

9. **Bignell E**, **Cairns TC**, **Throckmorton K**, **Nierman WC**, **Keller NP**. 2016. Secondary metabolite arsenal of an opportunistic pathogenic fungus. Phil Trans R Soc B **371**:20160023–9.

10. **Sugui JA**, **Pardo J**, **Chang YC**, **Zarember KA**, **Nardone G**, **Galvez EM**, **Müllbacher A**, **Gallin JI**, **Simon MM**, **Kwon-Chung KJ**. 2007. Gliotoxin is a virulence factor of Aspergillus fumigatus: gliP deletion attenuates virulence in mice immunosuppressed with hydrocortisone. Eukaryotic Cell **6**:1562–1569.

11. **Spikes S**, **Xu R**, **Nguyen CK**, **Chamilos G**, **Kontoyiannis DP**, **Jacobson RH**, **Ejzykowicz DE**, **Chiang LY**, **Filler SG**, **May GS**. 2008. Gliotoxin production in Aspergillus fumigatus contributes to host-specific differences in virulence. J Infect Dis **197**:479–486.

12. **Cramer RA**, **Gamcsik MP**, **Brooking RM**, **Najvar LK**, **Kirkpatrick WR**, **Patterson TF**, **Balibar CJ**, **Graybill JR**, **Perfect JR**, **Abraham SN**, **Steinbach WJ**. 2006.

612 Disruption of a nonribosomal peptide synthetase in Aspergillus fumigatus eliminates
613 gliotoxin production. Eukaryotic Cell **5**:972–980.

614 13. **Kupfahl C**, **Heinekamp T**, **Geginat G**, **Ruppert T**, **Härtl A**, **Hof H**, **Brakhage AA**.
615 2006. Deletion ofFmethanal the gliP gene of Aspergillus fumigatus results in loss of
616 gliotoxin production but has no effect on virulence of the fungus in a low-dose mouse
617 infection model. Mol Microbiol **62**:292–302.

618 14. **Sugui JA**, **Pardo J**, **Chang YC**, **Müllbacher A**, **Zarember KA**, **Galvez EM**, **Brinster**
619 **L**, **Zerfas P**, **Gallin JI**, **Simon MM**, **Kwon-Chung KJ**. 2007. Role of laeA in the
620 Regulation of alb1, gliP, Conidial Morphology, and Virulence in Aspergillus fumigatus.
621 Eukaryotic Cell **6**:1552–1561.

622 15. **Bok JW**, **Balajee SA**, **Marr KA**, **Andes D**, **Nielsen KF**, **Frisvad JC**, **Keller NP**. 2005.
623 LaeA, a regulator of morphogenetic fungal virulence factors. Eukaryotic Cell **4**:1574–
624 1582.

625 16. **Lamoth F**. 2016. Aspergillus fumigatus-Related Species in Clinical Practice. Frontiers in
626 Microbiology **7**:683.

627 17. **Balajee SA**, **Kano R**, **Baddley JW**, **Moser SA**, **Marr KA**, **Alexander BD**, **Andes D**,
628 **Kontoyiannis DP**, **Perrone G**, **Peterson S**, **Brandt ME**, **Pappas PG**, **Chiller T**. 2009.
629 Molecular identification of Aspergillus species collected for the Transplant-Associated
630 Infection Surveillance Network. J Clin Microbiol **47**:3138–3141.

631 18. **Alastruey-Izquierdo A**, **Mellado E**, **Peláez T**, **Pemán J**, **Zapico S**, **Alvarez M**,
632 **Rodríguez-Tudela JL**, **Cuenca-Estrella M**, **FILPOP Study Group**. 2013. Population-
633 based survey of filamentous fungi and antifungal resistance in Spain (FILPOP Study).
634 Antimicrob Agents Chemother **57**:3380–3387.

635 19. **van der Linden JWM**, **Arendrup MC**, **Warris A**, **Lagrou K**, **Pelloux H**, **Hauser PM**,
636 **Chryssanthou E**, **Mellado E**, **Kidd SE**, **Tortorano AM**, **Dannaoui E**, **Gaustad P**,
637 **Baddley JW**, **Uekötter A**, **Lass-Flörl C**, **Klimko N**, **Moore CB**, **Denning DW**,
638 **Pasqualotto AC**, **Kibbler C**, **Arikan-Akdagli S**, **Andes D**, **Meletiadis J**, **Naumiuk L**,
639 **Nucci M**, **Melchers WJG**, **Verweij PE**. 2015. Prospective multicenter international
640 surveillance of azole resistance in Aspergillus fumigatus. Emerging Infect Dis **21**:1041–
641 1044.

642 20. **Mellado E**, **Alcazar-Fuoli L**, **García-Effrón G**, **Alastruey-Izquierdo A**, **Cuenca-**
643 **Estrella M**, **Rodríguez-Tudela JL**. 2006. New resistance mechanisms to azole drugs
644 inAspergillus fumigatusand emergence of antifungal drugs-resistantA. fumigatusatypical
645 strains. Med Mycol **44**:367–371.

646 21. **Rokas A**, **Payne G**, **Fedorova ND**, **Baker SE**, **Machida M**, **Yu J**, **Georgianna DR**,
647 **Dean RA**, **Bhatnagar D**, **Cleveland TE**, **Wortman JR**, **Maiti R**, **Joardar V**, **Amedeo P**,
648 **Denning DW**, **Nierman WC**. 2007. What can comparative genomics tell us about species
649 concepts in the genus Aspergillus? Stud Mycol **59**:11–17.

22. **Hong S-B**, **Kim D-H**, **Park I-C**, **Samson RA**, **Shin H-D**. 2010. Isolation and Identification of AspergillusSection FumigatiStrains from Arable Soil in Korea. Mycobiology **38**:1.

23. **Frąc M**, **Jezierska-Tys S**, **YAGUCHI T**. 2015. Occurrence, Detection, and Molecular and Metabolic Characterization of Heat- Resistant Fungi in Soils and Plants and Their Risk to Human HealthAdvances in Agronomy. Elsevier Ltd.

24. **Tong X**, **Xu H**, **Zou L**, **Cai M**, **Xu X**, **Zhao Z**, **Xiao F**, **Li Y**. 2017. High diversity of airborne fungi in the hospital environment as revealed by meta-sequencing-based microbiome analysis. Sci Rep **7**:39606.

25. **Fedorova ND**, **Khaldi N**, **Joardar VS**, **Maiti R**, **Amedeo P**, **Anderson MJ**, **Crabtree J**, **Silva JC**, **Badger JH**, **Albarraq A**, **Angiuoli S**, **Bussey H**, **Bowyer P**, **Cotty PJ**, **Dyer PS**, **Egan A**, **Galens K**, **Fraser-Liggett CM**, **Haas BJ**, **Inman JM**, **Kent R**, **Lemieux S**, **Malavazi I**, **Orvis J**, **Roemer T**, **Ronning CM**, **Sundaram JP**, **Sutton G**, **Turner G**, **Venter JC**, **White OR**, **Whitty BR**, **Youngman P**, **Wolfe KH**, **Goldman GH**, **Wortman JR**, **Jiang B**, **Denning DW**, **Nierman WC**. 2008. Genomic islands in the pathogenic filamentous fungus Aspergillus fumigatus. PLoS Genet **4**:e1000046.

26. **Summerbell RC**, **de Repentigny L**, **Chartrand C**, **St Germain G**. 1992. Graft-related endocarditis caused by Neosartorya fischeri var. spinosa. J Clin Microbiol **30**:1580–1582.

27. **Lonial S**, **Williams L**, **Carrum G**, **Ostrowski M**, **McCarthy P**. 1997. Neosartorya fischeri: an invasive fungal pathogen in an allogeneic bone marrow transplant patient. Bone Marrow Transplant **19**:753–755.

28. **Gerber J**, **Chomicki J**, **Brandsberg JW**, **Jones R**, **Hammerman KJ**. 1973. Pulmonary aspergillosis caused by Aspergillus fischeri var. spinosus: report of a case and value of serologic studies. Am J Clin Pathol **60**:861–866.

29. **Coriglione G**, **Stella G**, **Gafa L**, **Spata G**, **Oliveri S**, **Padhye AA**, **Ajello L**. 1990. Neosartorya fischeri var fischeri (Wehmer) Malloch and Cain 1972 (anamorph: Aspergillus fischerianus Samson and Gams 1985) as a cause of mycotic keratitis. Eur J Epidemiol **6**:382–385.

30. **Abers MS**, **Ghebremichael MS**, **Timmons AK**, **Warren HS**, **Poznansky MC**, **Vyas JM**. 2016. A Critical Reappraisal of Prolonged Neutropenia as a Risk Factor for Invasive Pulmonary Aspergillosis. Open Forum Infect Dis **3**:ofw036.

31. **Beattie SR**, **Mark KMK**, **Thammahong A**, **Ries LNA**, **Dhingra S**, **Caffrey-Carr AK**, **Cheng C**, **Black CC**, **Bowyer P**, **Bromley MJ**, **Obar JJ**, **Goldman GH**, **Cramer RA**. 2017. Filamentous fungal carbon catabolite repression supports metabolic plasticity and stress responses essential for disease progression. PLoS Pathog **13**:e1006340–29.

32. **Kowalski CH**, **Beattie SR**, **Fuller KK**, **McGurk EA**, **Tang Y-W**, **Hohl TM**, **Obar JJ**, **Cramer RA**. 2016. Heterogeneity among Isolates Reveals that Fitness in Low Oxygen Correlates with Aspergillus fumigatus Virulence. mBio **7**.

33. **Childers DS**, **Raziunaite I**, **Mol Avelar G**, **Mackie J**, **Budge S**, **Stead D**, **Gow NAR**, **Lenardon MD**, **Ballou ER**, **MacCallum DM**, **Brown AJP**. 2016. The Rewiring of Ubiquitination Targets in a Pathogenic Yeast Promotes Metabolic Flexibility, Host Colonization and Virulence. PLoS Pathog **12**:e1005566.

34. **Sandai D**, **Yin Z**, **Selway L**, **Stead D**, **Walker J**, **Leach MD**, **Bohovych I**, **Ene IV**, **Kastora S**, **Budge S**, **Munro CA**, **Odds FC**, **Gow NAR**, **Brown AJP**. 2012. The evolutionary rewiring of ubiquitination targets has reprogrammed the regulation of carbon assimilation in the pathogenic yeast Candida albicans. mBio **3**.

35. **Houbraken J**, **Weig M**, **Groß U**, **Meijer M**, **Bader O**. 2016. Aspergillus oerlinghausenensis, a new mould species closely related to A. fumigatus. FEMS Microbiol Lett **363**:fnv236.

36. **Salichos L**, **Rokas A**. 2011. Evaluating ortholog prediction algorithms in a yeast model clade. PLoS ONE **6**:e18755.

37. **Abad A**, **Fernández-Molina JV**, **Bikandi J**, **Ramírez A**, **Margareto J**, **Sendino J**, **Hernando FL**, **Pontón J**, **Garaizar J**, **Rementeria A**. 2010. What makes Aspergillus fumigatus a successful pathogen? Genes and molecules involved in invasive aspergillosis. Rev Iberoam Micol **27**:155–182.

38. **Kjærbølling I**, **Vesth TC**, **Frisvad JC**, **Nybo JL**, **Theobald S**, **Kuo A**, **Bowyer P**, **Matsuda Y**, **Mondo S**, **Lyhne EK**, **Kogle ME**, **Clum A**, **Lipzen A**, **Salamov A**, **Ngan CY**, **Daum C**, **Chiniquy J**, **Barry K**, **LaButti K**, **Haridas S**, **Simmons BA**, **Magnuson JK**, **Mortensen UH**, **Larsen TO**, **Grigoriev IV**, **Baker SE**, **Andersen MR**. 2018. Linking secondary metabolites to gene clusters through genome sequencing of six diverse Aspergillus species. Proc Natl Acad Sci USA.

39. **Blin K**, **Wolf T**, **Chevrette MG**, **Lu X**, **Schwalen CJ**, **Kautsar SA**, **Suarez Duran HG**, **de los Santos ELC**, **Kim HU**, **Nave M**, **Dickschat JS**, **Mitchell DA**, **Shelest E**, **Breitling R**, **Takano E**, **Lee SY**, **Weber T**, **Medema MH**. 2017. antiSMASH 4.0—improvements in chemistry prediction and gene cluster boundary identification. Nucleic Acids Res **45**:W36–W41.

40. **Lind AL**, **Wisecaver JH**, **Lameiras C**, **Wiemann P**, **Palmer JM**, **Keller NP**, **Rodrigues F**, **Goldman GH**, **Rokas A**. 2017. Drivers of genetic diversity in secondary metabolic gene clusters within a fungal species. PLoS Biol **15**:e2003583.

41. **Gardiner DM**, **Howlett BJ**. 2005. Bioinformatic and expression analysis of the putative gliotoxin biosynthetic gene cluster of Aspergillus fumigatus. FEMS Microbiol Lett **248**:241–248.

42. **Frisvad JC**, **Larsen TO**. 2016. Extrolites of Aspergillus fumigatus and Other Pathogenic Species in Aspergillus Section Fumigati. Frontiers in Microbiology **6**:1485.

43. **Wiemann P**, **Guo C-J**, **Palmer JM**, **Sekonyela R**, **Wang CCC**, **Keller NP**. 2013. Prototype of an intertwined secondary-metabolite supercluster. Proc Natl Acad Sci USA **110**:17065–17070.

44. **El-Elimat T**, **Raja HA**, **Day CS**, **Chen W-L**, **Swanson SM**, **Oberlies NH**. 2014. Greensporones: Resorcylic Acid Lactones from an Aquatic Halenosporasp. J Nat Prod **77**:2088–2098.

45. **El-Elimat T**, **Raja HA**, **Figueroa M**, **Falkinham JO**, **Oberlies NH**. 2014. Isochromenones, isobenzofuranone, and tetrahydronaphthalenes produced by Paraphoma radicina, a fungus isolated from a freshwater habitat. Phytochemistry **104**:114–120.

46. **El-Elimat T**, **Raja HA**, **Day CS**, **McFeeters H**, **McFeeters RL**, **Oberlies NH**. 2017. α-Pyrone derivatives, tetra/hexahydroxanthones, and cyclodepsipeptides from two freshwater fungi. Bioorg Med Chem **25**:795–804.

47. **Raja HA**, **Paguigan ND**, **Fournier J**, **Oberlies NH**. 2017. Additions to <Emphasis Type="Italic">Lindgomyces</Emphasis> (Lindgomycetaceae, Pleosporales, Dothideomycetes), including two new species occurring on submerged wood from North Carolina, USA, with notes on secondary metabolite profiles. Mycol Progress **16**:535–552.

48. **Rivera-Chávez J**, **Raja HA**, **Graf TN**, **Gallagher JM**, **Metri P**, **Xue D**, **Pearce CJ**, **Oberlies NH**. 2017. Prealamethicin F50 and related peptaibols from Trichoderma arundinaceum: Validation of their authenticity via in situ chemical analysis. RSC Adv **7**:45733–45751.

49. **Sanchez JF**, **Somoza AD**, **Keller NP**, **Wang CCC**. 2012. Advances in Aspergillus secondary metabolite research in the post-genomic era. Nat Prod Rep **29**:351–371.

50. **Bode HB**, **Bethe B**, **Höfs R**, **Zeeck A**. 2002. Big effects from small changes: possible ways to explore nature's chemical diversity. Chembiochem **3**:619–627.

51. **Vandermolen KM**, **Raja HA**, **El-Elimat T**, **Oberlies NH**. 2013. Evaluation of culture media for the production of secondary metabolites in a natural products screening program. AMB Express **3**:71.

52. **Hemphill CFP**, **Sureechatchaiyan P**, **Kassack MU**, **Orfali RS**, **Lin W**, **Daletos G**, **Proksch P**. 2017. OSMAC approach leads to new fusarielin metabolites from Fusarium tricinctum. J Antibiot **70**:726–732.

53. **Frisvad JC**, **Andersen B**, **Thrane U**. 2008. The use of secondary metabolite profiling in chemotaxonomy of filamentous fungi. Mycol Res **112**:231–240.

54. **Eamvijarn A**, **Gomes NM**, **Dethoup T**, **Buaruang J**, **Manoch L**, **Silva A**, **Pedro M**, **Marini I**, **Roussis V**, **Kijjoa A**. 2013. Bioactive meroditerpenes and indole alkaloids from the soil fungus Neosartorya fischeri (KUFC 6344), and the marine-derived fungi Neosartorya laciniosa (KUFC 7896) and Neosartorya tsunodae (KUFC 9213). Tetrahedron **69**:8583–8591.

761 55. **Kimura Y**, **Hamasaki T**, **Nakajima H**, **Isogai A**. 1982. Structure of aszonalenin, a new
762 metabolite of aspergillus zonatus. Tetrahedron Letters **23**:225–228.

763 56. **Ruchti J**, **Carreira EM**. 2014. Ir-Catalyzed Reverse Prenylation of 3-Substituted Indoles:
764 Total Synthesis of (+)-Aszonalenin and (−)-Brevicompanine B. J Am Chem Soc
765 **136**:16756–16759.

766 57. **Ellestad GA**, **Mirando P**, **Kunstmann MP**. 1973. Structure of the metabolite LL-
767 S490.beta. from an unidentified Aspergillus species. J Org Chem **38**:4204–4205.

768 58. **Yamazaki M**, **Fujimoto H**, **Kawasaki T**. 1980. Chemistry of tremorogenic metabolites.
769 I. Fumitremorgin A from Aspergillus fumigatus. Chem Pharm Bull **28**:245–254.

770 59. **Feng Y**, **Holte D**, **Zoller J**, **Umemiya S**, **Simke LR**, **Baran PS**. 2015. Total Synthesis of
771 Verruculogen and Fumitremorgin A Enabled by Ligand-Controlled C–H Borylation. J Am
772 Chem Soc **137**:10160–10163.

773 60. **Pohland AE**, **Schuller PL**, **Steyn PS**, **Van Egmond HP**. 1982. Physicochemical data for
774 some selected mycotoxins. Pure and Applied Chemistry **54**:2219–2284.

775 61. **Afiyatullov SS**, **Kalinovskii AI**, **Pivkin MV**, **Dmitrenok PS**, **Kuznetsova TA**. 2005.
776 Alkaloids from the Marine Isolate of the Fungus Aspergillus fumigatus. Chemistry of
777 Natural Compounds **41**:236–238.

778 62. **Mundt K**, **Wollinsky B**, **Ruan H-L**, **Zhu T**, **Li S-M**. 2012. Identification of the
779 verruculogen prenyltransferase FtmPT3 by a combination of chemical, bioinformatic and
780 biochemical approaches. Chembiochem **13**:2583–2592.

781 63. **Fayos J**, **Lokensgard D**, **Clardy J**, **Cole RJ**, **Kirksey JW**. 1974. Letter: Structure of
782 verruculogen, a tremor producing peroxide from Penicillium verruculosum. J Am Chem
783 Soc **96**:6785–6787.

784 64. **Fill TP**, **Asenha HBR**, **Marques AS**, **Ferreira AG**, **Rodrigues-Fo E**. 2013. Time course
785 production of indole alkaloids by an endophytic strain of Penicillium brasilianum
786 cultivated in rice. Nat Prod Res **27**:967–974.

787 65. **Bok JW**, **Keller NP**. 2004. LaeA, a regulator of secondary metabolism in Aspergillus spp.
788 Eukaryotic Cell **3**:527–535.

789 66. **Hoff B**, **Kamerewerd J**, **Sigl C**, **Mitterbauer R**, **Zadra I**, **Kürnsteiner H**, **Kück U**.
790 2010. Two components of a velvet-like complex control hyphal morphogenesis,
791 conidiophore development, and penicillin biosynthesis in Penicillium chrysogenum.
792 Eukaryotic Cell **9**:1236–1250.

793 67. **Wiemann P**, **Brown DW**, **Kleigrewe K**, **Bok JW**, **Keller NP**, **Humpf H-U**, **Tudzynski**
794 **B**. 2010. FfVel1 and FfLae1, components of a velvet-like complex in Fusarium fujikuroi,
795 affect differentiation, secondary metabolism and virulence. Mol Microbiol **77**:972–994.

68. **O'Hanlon KA**, **Gallagher L**, **Schrettl M**, **Jöchl C**, **Kavanagh K**, **Larsen TO**, **Doyle S**. 2012. Nonribosomal Peptide Synthetase Genes pesLand pes1Are Essential for Fumigaclavine C Production in Aspergillus fumigatus. Appl Environ Microbiol **78**:3166–3176.

69. **Yu W**, **Pan Z**, **Zhu Y**, **An F**, **Lu Y**. 2017. Fumigaclavine C exhibits anti-inflammatory effects by suppressing high mobility group box protein 1 relocation and release. European Journal of Pharmacology **812**:234–242.

70. **Lind AL**, **Wisecaver JH**, **Smith TD**, **Feng X**, **Calvo AM**, **Rokas A**. 2015. Examining the evolution of the regulatory circuit controlling secondary metabolism and development in the fungal genus Aspergillus. PLoS Genet **11**:e1005096.

71. **Sáenz JP**, **Grosser D**, **Bradley AS**, **Lagny TJ**, **Lavrynenko O**, **Broda M**, **Simons K**. 2015. Hopanoids as functional analogues of cholesterol in bacterial membranes. Proc Natl Acad Sci USA **112**:11971–11976.

72. **Li S-M**. 2010. Genome mining and biosynthesis of fumitremorgin-type alkaloids in ascomycetes. J Antibiot **64**:45–49.

73. **Kale SP**, **Milde L**, **Trapp MK**, **Frisvad JC**, **Keller NP**, **Bok JW**. 2008. Requirement of LaeA for secondary metabolism and sclerotial production in Aspergillus flavus. Fungal Genetics and Biology **45**:1422–1429.

74. **Perrin RM**, **Fedorova ND**, **Bok JW**, **Cramer RA**, **Wortman JR**, **Kim HS**, **Nierman WC**, **Keller NP**. 2007. Transcriptional regulation of chemical diversity in Aspergillus fumigatus by LaeA. PLoS Pathog **3**:e50.

75. **Madden T**. 2013. The BLAST Sequence Analysis Tool. *In* The NCBI Handbook [Internet]. 2nd edition. National Center for Biotechnology Information (US).

76. **Micallef L**, **Rodgers P**. 2014. eulerAPE: Drawing Area-Proportional 3-Venn Diagrams Using Ellipses. PLoS ONE **9**:e101717–18.

77. **Stajich JE**, **Harris T**, **Brunk BP**, **Brestelli J**, **Fischer S**, **Harb OS**, **Kissinger JC**, **Li W**, **Nayak V**, **Pinney DF**, **Stoeckert CJ**, **Roos DS**. 2012. FungiDB: an integrated functional genomics database for fungi. Nucleic Acids Res **40**:D675–81.

78. **Supek F**, **Bošnjak M**, **Škunca N**, **Šmuc T**. 2011. REVIGO summarizes and visualizes long lists of gene ontology terms. PLoS ONE **6**:e21800.

79. **Krzywinski M**, **Schein J**, **Birol I**, **Connors J**, **Gascoyne R**, **Horsman D**, **Jones SJ**, **Marra MA**. 2009. Circos: an information aesthetic for comparative genomics. Genome Res **19**:1639–1645.

80. **Sullivan MJ**, **Petty NK**, **Beatson SA**. 2011. Easyfig: a genome comparison visualizer. Bioinformatics **27**:1009–1010.

81. **El-Elimat T**, **Figueroa M**, **Ehrmann BM**, **Cech NB**, **Pearce CJ**, **Oberlies NH**. 2013. High-resolution MS, MS/MS, and UV database of fungal secondary metabolites as a dereplication protocol for bioactive natural products. J Nat Prod **76**:1709–1716.

82. **Paguigan ND**, **El-Elimat T**, **Kao D**, **Raja HA**, **Pearce CJ**, **Oberlies NH**. 2017. Enhanced dereplication of fungal cultures via use of mass defect filtering. J Antibiot **70**:553–561.

83. **Colot HV**, **Park G**, **Turner GE**, **Ringelberg C**, **Crew CM**, **Litvinkova L**, **Weiss RL**, **Borkovich KA**, **Dunlap JC**. 2006. A high-throughput gene knockout procedure for Neurospora reveals functions for multiple transcription factors. Proc Natl Acad Sci USA **103**:10352–10357.

84. **Malavazi I**, **Goldman GH**. 2012. Gene disruption in Aspergillus fumigatus using a PCR-based strategy and in vivo recombination in yeast. Methods Mol Biol **845**:99–118.

85. **Schiestl RH**, **Gietz RD**. 1989. High efficiency transformation of intact yeast cells using single stranded nucleic acids as a carrier. Curr Genet **16**:339–346.

86. **Goldman GH**, **Reis Marques dos E**, **Duarte Ribeiro DC**, **de Souza Bernardes LA**, **Quiapin AC**, **Vitorelli PM**, **Savoldi M**, **Semighini CP**, **de Oliveira RC**, **Nunes LR**, **Travassos LR**, **Puccia R**, **Batista WL**, **Ferreira LE**, **Moreira JC**, **Bogossian AP**, **Tekaia F**, **Nobrega MP**, **Nobrega FG**, **Goldman MHS**. 2003. Expressed sequence tag analysis of the human pathogen Paracoccidioides brasiliensis yeast phase: identification of putative homologues of Candida albicans virulence and pathogenicity genes. Eukaryotic Cell **2**:34–48.

87. **Sambrook J**, **Russell DW**. 2001. Molecular Cloning, 3rd ed. Cold Spring Harbor Laboratory Press, London.

88. **Yin W-B**, **Grundmann A**, **Cheng J**, **Li S-M**. 2009. Acetylaszonalenin biosynthesis in Neosartorya fischeri. Identification of the biosynthetic gene cluster by genomic mining and functional proof of the genes by biochemical investigation. J Biol Chem **284**:100–109.

857 **Tables**

858

859 **Table 1. *A. fischeri* shows enhanced resistance relative to *A. fumigatus* for several**

860 **antifungal drugs.**

Strain	Posaconazole [µg/ml]	Voriconazole [µg/ml]	Itraconazole [µg/ml]	Caspofungin [µg/ml]
A. fumigatus	0.7	0.8	5	0.09
A. fischeri	2.4	> 4	> 24	0.06

861

Figure Legends

Figure 1: *A. fischeri* is significantly less virulent than *A. fumgiatus* in multiple models of IPA. AB) Cumulative survival of mice inoculated with 1e5 (A) or 2e6 (B) conidia in a leukopenic model of IPA. A) n=10/group B) n=12/group, 4/PBS. *p=0.0098 by Log-Rank test, p=0.0002 by Gehan-Breslow-Wilcoxon test. C) Cumulative survival of mice inoculated with 2e6 conidia in a triamcinolone model of IPA. n=12/group, 4/PBS. *p=<0.0001 by Log-Rank and Gehan-Breslow-Wilcoxan tests. D) Histological sections from 3 days post inoculation in a triamcinolone model of IPA stained with H&E and GMS. Images were acquired at 100x. EF) Cumulative survival of *G. mellonella* larvae inoculated with 1e6 (E) or 1e9 (F) conidia. 10 larvae were used per condition in all assays.

Figure 2: Radial growth curves of CEA10 (*A. fumigatus*) or NRRL181 (*A. fischeri*) at 37°C. 1e3 conidia were point inoculated on each plate then plates were incubated at 37°C in normoxia (N; ~21% oxygen, 5%CO_2) or hypoxia (H; 0.2% O_2, 5%CO_2); colony diameter was measured every 24 hours. Mean and SEM of triplicates. CAA – Casamino acids; GMM – glucose minimal media.

Figure 3: Host-relevant stress phenotypes of *A. fumigatus* and *A. fischeri*. A) Fitness ratio of *A. fumigatus* or *A. fischeri* in hypoxia as measured by dry weight of hypoxia cultures divided by dry weight of normoxia cultures. Data represents mean and SEM of biological triplicates; ***p=0.0006 by Student's t-test. B) Growth inhibition of strains grown on 1% lactate minimal media with 0.1% 2-deoxyglucose (2-DG) under a range of low oxygen conditions. C) *A. fumigatus* and *A. fischeri* were grown in the presence of the cell wall perturbing agent Congo

885 Red (0.5mg/mL), the oxidative stressor Menadione (20 µM), or the chitin perturbing agent
886 calcofluor white (CFW, 25µg/mL). Plates were grown for 96 hours at 37°C and 5% CO_2. For all
887 plates except Congo Red and its GMM control, 1e3 spores were plated. For Congo red and the
888 control GMM plate 1e5 spores were plated. Student's t-test was performed where *: $p<0.05$, **:
889 $p<0.01$. D) Strains were grown for 48 h at 37°C in liquid complete medium supplemented with
890 increasing concentrations of H_2O_2.
891
892 **Figure 4: Secondary Metabolite Clusters of *A. fumigatus* and *A. fisheri* have diverged**
893 **during their evolution.** Predicted secondary metabolite gene clusters are shown in the inner
894 track, are alternatively colored dark and light gray, and their size is proportional to the number of
895 genes in them. Black ticks on the exterior of the cluster track indicate a gene that possesses an
896 ortholog in the other species but is not in a secondary metabolite gene cluster in the second
897 species. White dots indicate species-specific clusters. Solid bars on the exterior correspond to the
898 chromosome on which the clusters below them reside. Genes are connected to their orthologs in
899 the other species with dark lines if >90% of the cluster genes in *A. fumigatus* are conserved in the
900 same cluster in *A. fischeri*. Lighter lines connect all other orthologs that are present in both
901 species' sets of secondary metabolite clusters. Image was made using Circos version 0.69-4 (79).
902
903 **Figure 5: Secondary metabolite production in *A. fischeri*.** A) Compounds isolated from *A.*
904 *fischeri*: **(1)** sartorypyrone A, **(2)** sartorypyrone E, **(3)** 14-epimer aszonapyrone A, **(4)**
905 aszonalenin, **(5)** acetylaszonalenin, **(6)** fumitremorgin A, **(7)** fumitremorgin B, **(8)** verruculogen,
906 **(9)** C-11 epimer verruculogen TR2, and **(10)** 13-*O*-prenyl-fumitremorgin B. The color coding
907 indicates which putative class the molecule belongs to; e.g., terpenes, PKS, or NRPS. B) Top,

908 *Aspergillus fischeri* was initially grown on rice for two weeks, and then extracted using methods
909 outlined in Fig. S6. The rice culture yielded compounds **1**, **4**, and **5**. Middle, *A. fischeri* was
910 grown on multigrain Cheerios for two weeks, which yielded compounds **1** and **4**-**9**. Bottom, *A.*
911 *fischeri* on Quaker oatmeal for two weeks. All compounds that were previously isolated in rice
912 and multigrain cheerios cultures in addition to three new compounds (**2**, **3**, and **10**) were found in
913 the oatmeal culture. All pictures depict fungi growing in 250 mL Erlenmeyer flasks; left panel
914 indicates top view, while the right panel shows bottom view. All chromatographic profiles have
915 been normalized to the highest μAU value. C) *Aspergillus fischeri* WT and Δ*laeA* were grown on
916 solid breakfast oatmeal for two weeks and extracted using organic solvents as indicated
917 previously. The crude de-sugared and de-fatted extracts were run using UPLC-MS at a
918 concentration of 2 mg/mL with 5 μL being injected for analysis. The chromatographic profiles
919 were normalized to the highest μAU value. Mass spec analysis indicated the presence of
920 secondary metabolites **1**–**10** within the wild type, and only **1**-**6**, **8**, and **9** were seen in the *ΔlaeA*
921 mutant. All pictures show *A. fischeri* grown on oatmeal agar in Petri plates.

Supplementary Material

Figure S1: Early growth in glucose minimal media (GMM) and lung homogenate media. *A. fumigatus* CEA10 or *A. fischeri* NRRL181 were cultured in flat-bottom 96 well plates at $2x10^4$ conidia per well. Conidia were added in a 20µL of 0.01% Tween-80 and media was carefully pipetted over the inoculum into each well. Lung homogenate was generated according to (31). Plates were incubated for 7 hours at 37°C before measurements at 405nm were taken every 10 min. Mean and SEM of eight technical replicates; data is representative of three biological replicates.

Figure S2: Radial growth curves of *A. fumigatus* CEA10 or *A. fischeri* NRRL181 at 30°C. 1e3 conidia were point inoculated on each plate then plates were incubated at 30°C in normoxia (~21% oxygen, 5%CO_2); colony diameter was measured every 24 hours. Mean and SEM of triplicates. Tween-80 – 1% Tween-80 provided as sole carbon source; CAA – Casamino acids; GMM – glucose minimal media.

Figure S3: Radial growth at 44°C. Error bars indicate standard deviations between biological duplicates (**P-value < 0.005 in a paired, equal variance student t-test).

Figure S4: Conserved and Species-Specific Proteins. Left, Venn diagram showing the sets of *A. fischeri*-specific proteins, shared orthologous proteins, and *A. fumigatus*-specific proteins encoded in each genome. Numbers below each species name indicate the total number of proteins encoded in that genome. Right, Venn diagram showing the sets of *A. fischeri*-specific secondary metabolite cluster proteins, shared secondary metabolite cluster genes, and *A.*

945 *fumigatus*-specific secondary metabolite cluster genes. Numbers below each species name
946 indicate the total number of secondary metabolite cluster proteins encoded in that genome. In
947 each diagram, circles are proportional to the number of proteins they contain.
948
949 **Figure S5: The acetylaszonalenin and gliotoxin clusters in *A. fumigatus* and *A. fischeri* are**
950 **located immediately next to one another.** The portions of Clusters 37 and 25 from *A. fischeri*
951 and *A. fumigatus*, respectively, that are known to contain the previously characterized
952 acetylaszonalenin (88) and gliotoxin (41) clusters is shown. Genes colored in shades of green are
953 involved in the acetylaszonalenin biosynthetic pathway. Dark green, *anaPS* (nonribosomal
954 peptide synthase). Light green, *anaAT* (acetyltransferase). Green, *anaPT* (prenyltransferase).
955 Orange, gliotoxin biosynthetic genes. Gray arrow, syntenic gene in both species not involved in
956 gliotoxin synthesis. Sequences that are similar to one another (based on blastn scores) are
957 marked by gray parallelograms. Image was made using EasyFig version 2.2.2 (80).
958
959 **Figure S6: Chemistry methods.** Approximately 60 mL of 1:1 methanol:chloroform was added
960 to cultures of *Aspergillus fischeri* grown on solid-state fermentation for two weeks. The cultures
961 were then chopped thoroughly with a large scalpel and shaken for 16 hours using an orbital
962 shaker. The liquid culture was then vacuum filtered and concentrated using 90 mL chloroform
963 and 150 mL water and transferred into a separatory funnel. The chloroform (bottom) layer was
964 drawn off and evaporated to dryness. The dried, de-sugared extract was reconstituted in 100 mL
965 of 1:1 methonal:acetonitrile and 100 mL of hexane. The biphasic solution was shaken vigorously
966 and transferred to a separatory funnel. The methonal:acetonitrile layer was evaporated to dryness
967 under vacuum, producing a de-fatted extract. The extract was then subdivided into several peaks

968 or fractions using flash chromatography. The subfractions were further separated using HPLC
969 until pure compounds were isolated. The pure compounds were subjected to UPLC-MS analysis
970 to establish the molecular formula and fragmentation patterns. Finally, pure compounds were
971 identified using both NMR analysis as well as information from UPLC-MS data.
972
973 **Figure S7: Media Study.** Base peak chromatograms as measured by LC-MS, illustrating how
974 the chemistry profiles varied based on growth conditions. PDA + ab was used as the chemical
975 control to observe the differences in the secondary metabolites, due to it being the media that *A.*
976 *fischeri* is stored. There were overall no chemical differences observed between the different
977 variations of PDA media. Each peak (which indicates different chemical entities) was observed
978 in the three PDA variations, albeit at fluctuating intensities. SDA, PYG, and YESD produced the
979 majority of the peaks observed in PDA, but it also lacked some observed peaks, indicating that
980 these growth conditions were not chemically favored. CYA produced the majority of the peaks,
981 as well as an additional peak that was observed at a much lower intensity in PDA. However, this
982 peak was similarly observed in OMA. OMA produced similar peaks to those observed in PDA,
983 but with higher intensity. Due to this, OMA was selected to further study. The gray boxes
984 indicate differences in the observed peaks compared to PDA. See Figshare document
985 (https://doi.org/10.6084/m9.figshare.7149167.v1) for more information.
986
987 **Figure S8: Southern blot confirming Δ*laeA* mutant.** A 1kb probe recognizes a single DNA
988 band (~4.4kb) in the wild type strain and a single DNA band (~2.7kb) in the Δ*laeA* mutant.
989
990 **Table S1: Virulence genes in *A. fumigatus* and *A. fischeri*.**

Table S2: Bioinformatically predicted secondary metabolite clusters in *A. fumigatus* strain CEA10.

Table S3: Bioinformatically predicted secondary metabolite clusters in *A. fischeri* strain NRRL 181.

Table S4: Different Types of Growth Media used for *Aspergillus fischeri*.

Figure 1

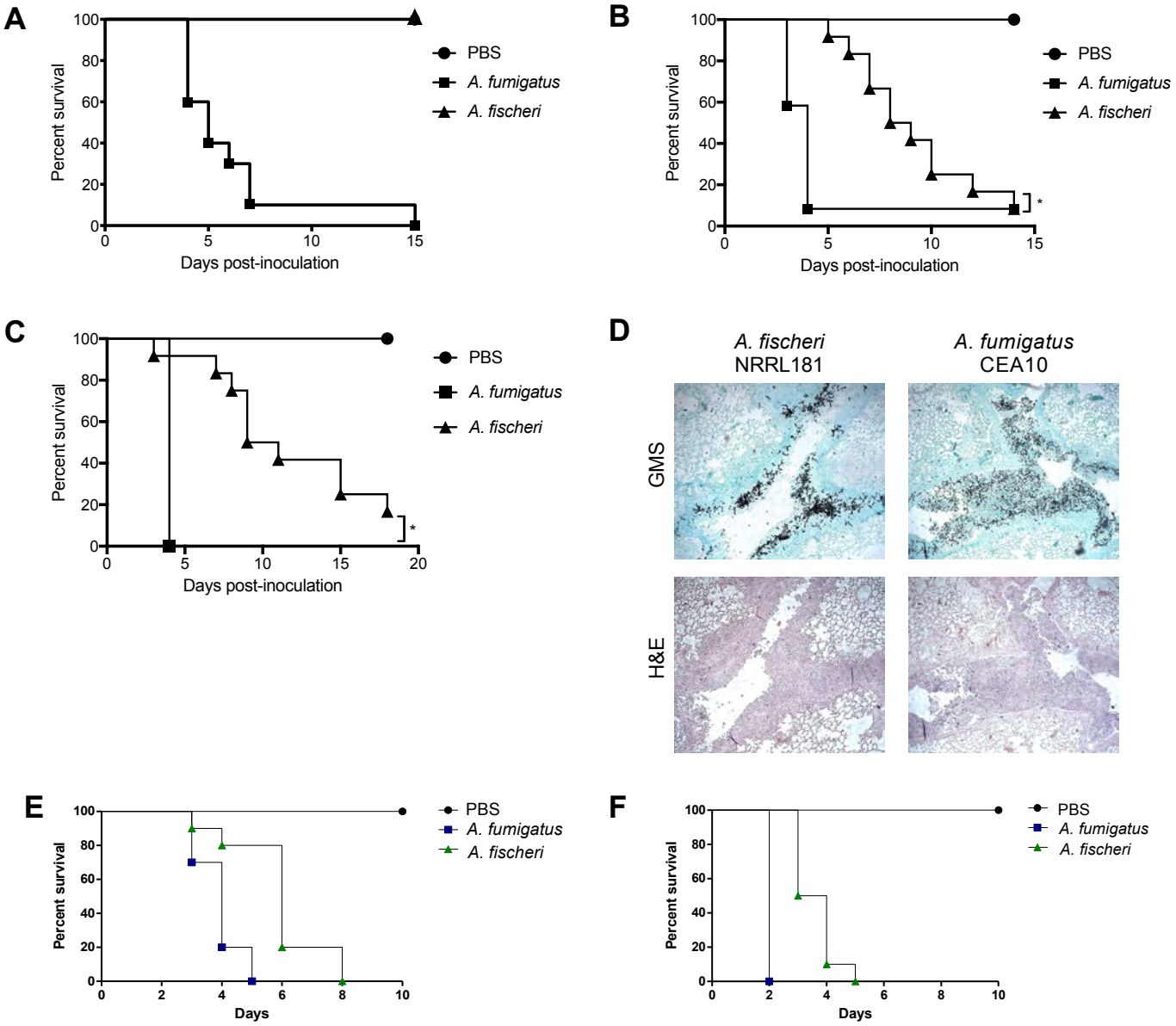

Figure 2

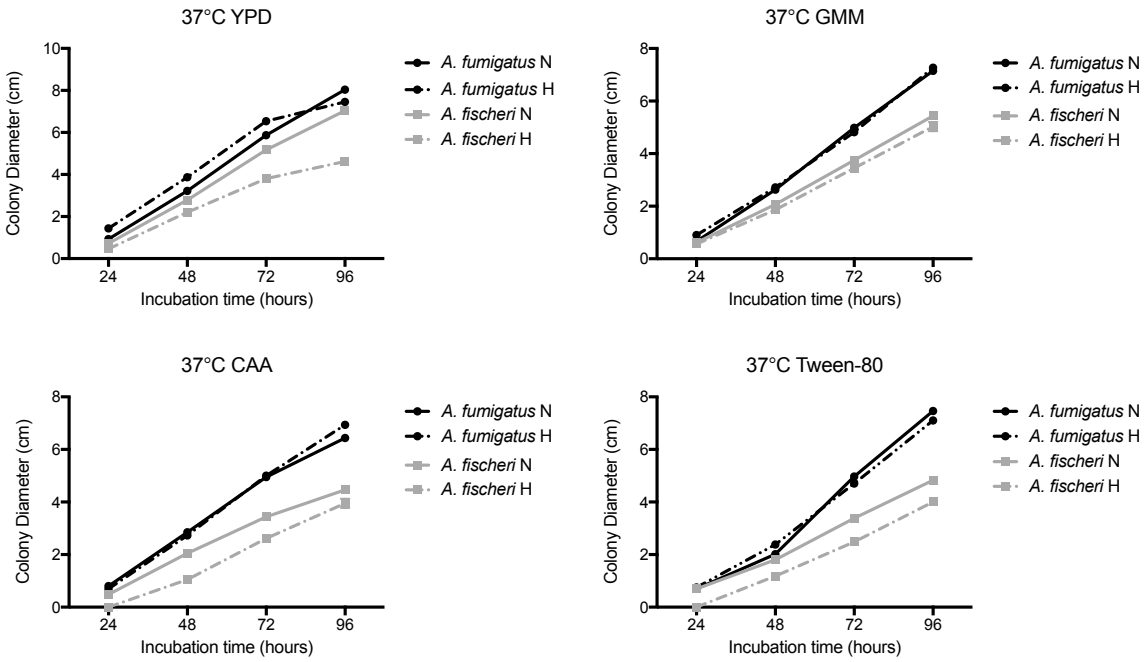

Figure 3

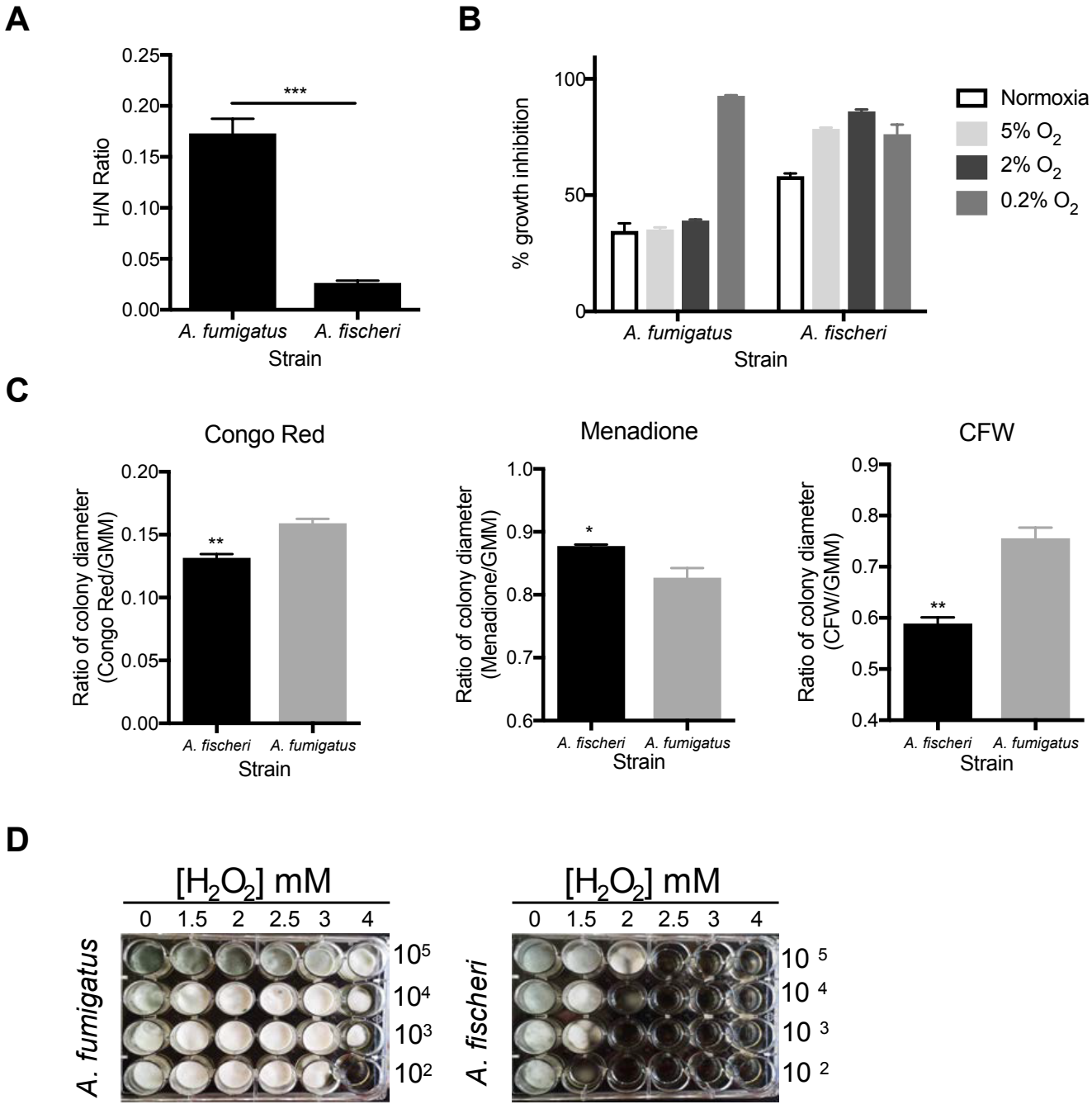

Figure 4

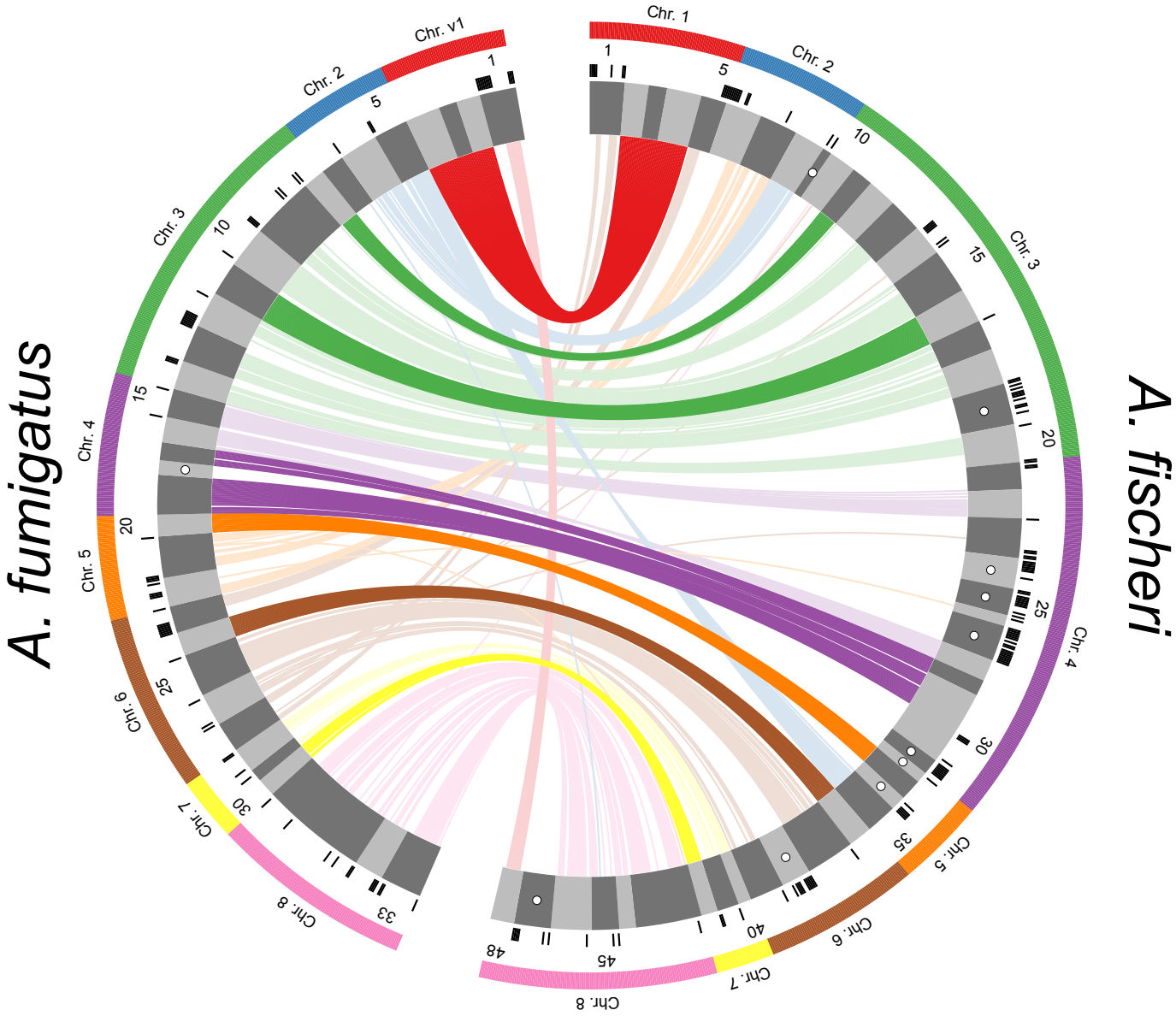

Figure 5

A

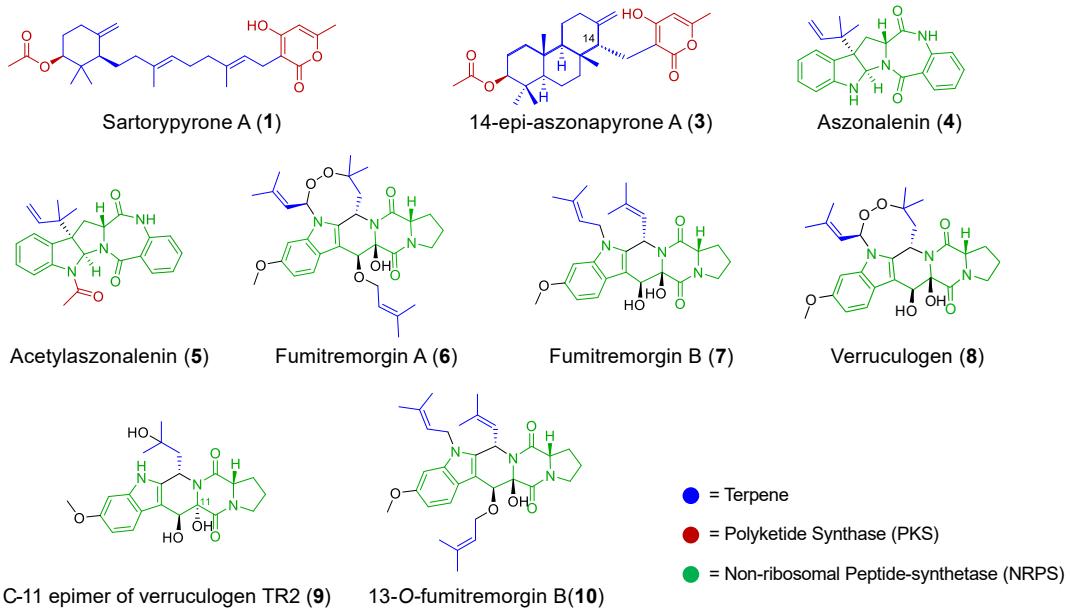

B

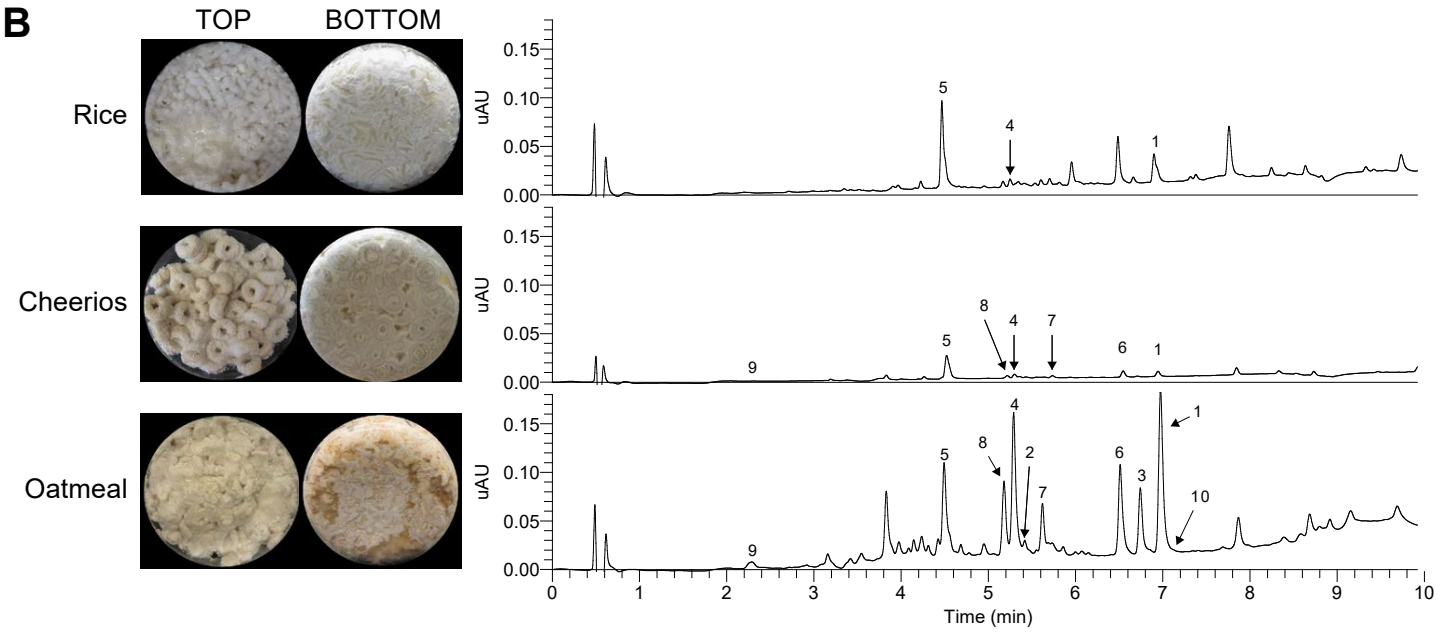

C